2011

Cr(VI)-induced malignant transformation of a bronchial epithelial cell line association with altered mitochondria and bioenergetic phenotypes

Ana Daniela F.P. Sampaio

DEPARTAMENTO DE CIÊNCIAS DA VIDA

FACULDADE DE CIÊNCIAS E TECNOLOGIA
UNIVERSIDADE DE COIMBRA

Cr(VI)-induced malignant transformation of a bronchial epithelial cell line association with altered mitochondria and bioenergetic phenotypes

Ana Daniela Ferreira Pinto Sampaio

2011

DEPARTAMENTO DE CIÊNCIAS DA VIDA

FACULDADE DE CIÊNCIAS E TECNOLOGIA
UNIVERSIDADE DE COIMBRA

Cr(VI)-induced malignant transformation of a bronchial epithelial cell line association with altered mitochondria and bioenergetic phenotypes

Dissertação apresentada à Universidade de Coimbra para cumprimento dos requisitos necessários à obtenção do grau de Mestre em Bioquímica, realizada sob a orientação científica da Doutora Maria Carmen Alpoim (Faculdade de Ciências e Tecnologia da Universidade de Coimbra).

Ana Daniela Ferreira Pinto Sampaio

2011

"Stones on the way?
I keep all.
Someday I'll make a castle ... "

Fernando Pessoa

“You may have to fight a battle more than once to win it.”

Margaret Thatcher

“…The best is yet to come”

Robert Browning

To my mother

Who never gave up

Acknowledgments

I want to express my acknowledgements to Dr. Carmen Alpoim, supervisor of the present work for her orientation through this year and knowledge. To Dr. Rui Carvalho for all the help, knowledge, patience and availability. To Dr. Ana Urbano for the availability and willingness. To Dr. Carlos Palmeira, Dr. Paulo Oliveira and Dr. Vilma Sardão for all the knowledge, availability and scientific cooperation. To Dr. Vera, Dr. Manolo, Margarida Abrantes, and Ana Cristina Gonçalves for the sympathy and goodwill.

I also want to thanks Ludgero for his availability and patience on all the long nights spend in NMR. To Carlos for teaching me all cell culture techniques and Luís for the LabMeetings and productive discussions. To Mrs. Amelia for all the friendship and help and also to all the people who loaned me material to be able to do my lab work and without it I would not have succeed.

And last but not least, to my parents for all their support, love, dedication and for always believing in me. To Vânia, Alexandre, Bé, Paula, Dinis e Carolina for their support, care and all the good moments of distraction! To all my friends made along this years for the fellowship and all the unforgettable moments. And for you Pedro, for all the love, for staying with me in the bad and good moments, for your dedication, patience, support and for always believing in me.

Index

List of Acronyms

ATP – Adenosine Triphosphate

BEAS-2B – Bronchial Epithelium Airway System 2B cells

BSA – Bovine Serum Albumine

CA - California

Calcein-AM - Calcein acetoxymethyl ester

CoA - coenzyme A

Cox (IV) - Cytochrome c oxidase subunit IV

DAPI - 4',6-diamidino-2-phenylindole

DMSO - Dimethyl sulfoxide

DNA – Desoxirribonucleic acid

EDTA - Ethylenediaminetetraacetic acid

ECCAC - European Collection of Cells Cultures

FBS - Fetal Bovine Serum

FITC - Fluorescein isothiocyanate

HCl - Hydrogen Chloride

Hoechst 33342 - trihydrochloride trihydrate

IARC - International Agency for Research on Cancer

JC-1 - 5,5',6,6'-tetrachloro-1,1',3,3'-tetraethyl benzimidazolcarbocyanine iodide

KCl - potassium chloride

KH_2PO_4 - Monopotassium phosphate

Mitotracker red - chloromethyl-X-rosamine

NaCl - Sodium chloride

Na_2HPO_4 - Disodium hydrogen phosphate

NaOH - Sodium hydroxide

NSCLC - Non-Small Cell Lung Carcinoma

PBS - Phosphate buffered saline

PBST - Phosphate Buffered Saline with Tween 20

SCC - Squamous Cell Carcinoma

SCLC - Small-Cell Lung Carcinoma

TMRM - Tetramethyl Rhodamine Methyl Ester

UCP2 - Mitochondrial uncoupling protein 2

USA – United States of America

WHO – World Health Organization

Abstract

Cancer is the main cause of death worldwide, it arises from a deregulation of homeostasis and is characterized by the growth of cells caused by a genetic and/or environmental cause, also designated neoplasia (Chiang A.C., 2008). According to the World Health Organization, lung cancer is the most common cause of cancer death in men and women worldwide (WHO, 2006). There are two main histological types of lung cancer, small-cell lung carcinoma (SCLC) and non-small cell lung carcinoma (NSCLC) (Wistuba I.I. & Gazdar, A.F. 2006).

Chromium (Cr) presents a wide range of oxidations states. The most common are Cr(0), Cr(III) and Cr(VI). The Chromium (VI) is a well known carcinogen playing an important role in lung carcinoma. It is one of the studied and investigated metals concerning to mutagenicity and carcinogenicity (Kondo, K. *et al.* 2003).

An *in vitro* study of malignant transformation of bronchial epithelial cells by Cr(VI) was already achieved in order to understand Cr(VI)-induced carcinogenesis, and an *in vitro* cellular model was established using BEAS-2B cells. This cells were exposed to 1μM Cr(VI) and changes in cell´s ploidy and a decrease in cloning efficiency was observed (Rodrigues *et al.*, 2009).

The genetic alterations that lead to tumors development are directly related to glycolysis, the way that cells react to hypoxia and the capacity of recruitment of new blood vessels (Dang C.V. and Semenza G.L., 1999). Mitochondria play important roles in cellular energy metabolism, defects in mitochondrial function have long been suspected to contribute to the development and progression of cancer. Certain malignant cells have also been reported to have alterations in mitochondrial content as compared to normal cells of the same tissue (Frezza and Gottlieb, 2009).

Resumo

O Cancro é a maior causa de morte a nível mundial, surge da desregulação da homeostase e é caracterizado pelo crescimento celular causado por factores ambientais e/ou genéticos, também designado por neoplasia (Chiang A.C., 2008). De acordo com a World Health Organization, o cancro do pulmão é a causa mais comum de morte em homens e mulheres mundialmente (WHO, 2006).

O Crómio (Cr) apresenta uma vasta gama de estados de oxidação. O mais comuns são Cr(0), Cr(III) e Cr(VI). O Crómio (VI) é um carcinogéneo bem conhecido que desempenha um papel importante nos carcinomas do pulmão. É um dos metais estudados e investigados sobre a mutagenicidade e carcinogenicidade (Kondo, K. *et al.*, 2003).

Um estudo *in vitro* de malignização de células epiteliais bronquiais com Cr(VI) foi realizado com o objectivo de entender a carcinogénese induzida por Cr(VI) e um modelo celular *in vitro* foi estabelecido utilizando células BEAS-2B. Estas células foram espostas a 1µM Cr(VI) sendo observadas alterações na poloidia das células e um decréscimo na eficiência de clonagem (Rodrigues *et al*., 2009).

As alterações genéticas que levam ao desenvolvimento de tumores estão directamente relacionadas com a glicólise, a maneira como as células reagem à hipóxia e a sua capacidade no recrutamento de novos vasos sanguíneos (Dang C.V. and Semenza G.L., 1999). A mitocôndria tem um papel importante no metabolismo energético celular, há muito tempo se suspeitava que defeitos na sua função contribuíam para o desenvolvimento e progressão de cancro. Algumas células malignizadas apresentam alterações no conteúdo mitocôndrial quando comparadas com células normais do mesmo tecido (Frezza and Gottlieb, 2009).

Introduction

1. Introduction

1.1 Respiratory System

The main purpose of respiration process is providing oxygen for the cells of the body. The respiratory system is the anatomical system that performs gas exchange, where molecules of oxygen and carbon dioxide are exchanged by diffusion, between the blood and the external environment. This process takes place in the alveolar region of the lungs. (Haton, A. *et al.* 2009). The carbon dioxide, a waste product of cellular function, is absorbed by the alveoli and expelled from the body during exhalation. The oxygen, important for our cells to live and function properly, is inhaled and transferred to the blood by the alveoli, toward the inside of bloodstream to the heart and other tissues of the body. Oxygen is also important for cellular respiration, the process by which molecules like glucose ($C_6H_{12}O_6$) and fatty acids are broken, giving rise to much simpler molecules of carbon dioxide (CO_2) and water (H_2O), to make energy in the form of adenosine triphosphate (ATP) (Whittemore S., 2004).

The respiratory system include the nose, pharynx, larynx, trachea, bronchi and lungs (see figure 1).

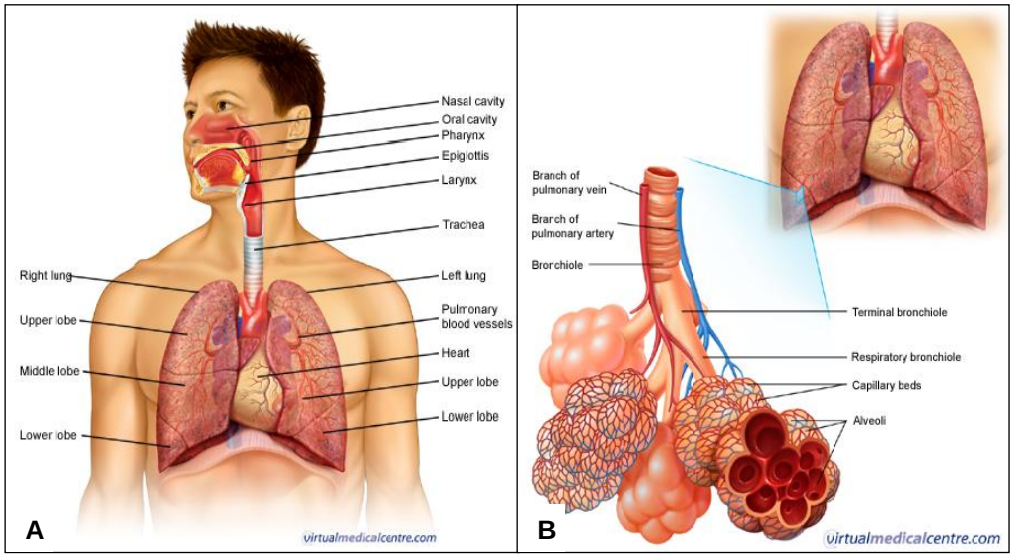

Figure 1 – A schematic view of the human respiratory system (A) and alveoli (B) (adapted from virtualmedicalcentre.com).

1.2 Cancer

Cancer arises from a deregulation of homeostasis and is characterized by the growth of cells caused by a genetic and/or environmental cause, also designated neoplasia. Metastases are the leading cause of death from cancer (WHO, 2010). Metastases are tumor lesions that invade non-adjacent organs. When a tumor spreads into neighbor organs it is called invasion, when spreads into distant organs, creates metastasis, making cancer so difficult to treat (Chiang A.C., 2008).

With respect to treatment, a primary tumor can be removed easily unless it invades an important organ or is nearby nerves or vessels.

Cancer is the main cause of death worldwide, responsible for 13% of all deaths, according to the World Health Organization. The most frequent body parts affected by this complex disease are lung, breast, colon and rectal (colorectal cancer) and stomach (WHO, 2010).

Carcinogenesis is related with self-sufficiency in growth signals, insensitivity to growth-inhibitory signals, evasion of apoptosis, limitless replicative potential, sustained angiogenesis and tissue invasion, and metastasis, also designated as the hallmarks of cancer (Hanahan and Weinberg, 2000). These hallmarks of cancer are related to deregulation of signaling pathways with the alteration of tumor suppressor genes as p53 or RB and oncogenes as RAS or c-MYC (Yeung *et al.*, 2008). Recent studies demonstrate that cancer cells have a high glycolytic rate, a phenotypic strategy in tumor progression and an evidence of the importance of the microenvironment in carcinogenic process (Gatenby and Gillies, 2004).

Recently was presented a 7th hallmark of cancer, the “Warburg effect”, in which cells, in the process to obtain energy, use glycolysis in stead of oxidative phosphorylation even in cases where oxygen is abundant (Yeung *et al.*, 2008).

1.3 Lung Cancer

According to the World Health Organization, lung cancer is the most common cause of cancer death in men and women worldwide, causing annually 1.3 million deaths. Lung cancer is characterized by an uncontrolled growth of abnormal cells in lung tissue. Primary lung cancers, which start in the lung, derive from epithelial cells and are also known as carcinomas (WHO, 2006). The highest rates of incidence in men are observed in Eastern Europe and North America. On the other hand, in women the highest incidence rates are observed in North America and in Europe, specifically in Northern and Western Europe. In the year 2000, it is estimated that the cases of lung cancer in Europe were around 375.000 cases, and the resulting deaths were 347.000, 280.000 men and 67.000 women. (Tyczynski J. E. et al., 2003).

The major cause of lung cancer is tobacco smoke and nonsmokers represent 15% of lung cancers (Thun, M.J. *et al.*, 2008). Environmental and occupational factors, diet, genetic factors and lung injury (as chronic obstructive pulmonary diseases and inflammatory/ fibrosing lung diseases) are also responsible for the appearance of lung cancers (Tomashefski J.F*. et. al* 2008).

1.3.1 Histological types of Lung Cancer

There are two main histological types of lung cancer, small-cell lung carcinoma (SCLC) and non-small cell lung carcinoma (NSCLC). Non-small cell lung carcinoma is also subdivided in three histological types: adenocarcinoma (including bronchioalveolar carcinoma), squamous cell carcinoma (SCC), and large cell carcinoma (Wistuba I.I. & Gazdar, A.F. 2006). According to “The International Agency for Research on Cancer” (IARC) non-small cell lung carcinoma represents the leading type of the cases of lung cancer (Tomashefski J.F*. et. al* 2008).

According to the World Health Organization (WHO) classification, adenocarcinomas are, in turn, subdivided in other subtypes: bronchioalveolar carcinoma, non bronchioalveolar adenocarcinoma, papillary, micropapillary, acinar, solid adenocarcinoma with mucin production and mixed adenocarcinoma (the most common histological form with multiple morphologies). Adenocarcinomas are characterized as malignant epithelial tumors with glandular differentiation or mucin production. (Tomashefski J.F*. et. al.* 2008).

1.4 Chromium (Cr)

Chromium (Cr) presents a wide range of oxidations states. The most common are Cr(0), Cr(III) and Cr(VI). Cr(0) is considered inert because of is rather resistance to oxidation by atmospheric oxygen. It is used with other metals, as Cobalt (Co), Iron (Fe) and Nickel (Ni). Some studies suggest that medical prostheses containing Cr(0) can slowly release the more soluble and reactive Cr(III) and Cr(VI) states, which may explain the nonspecific irritation in the respiratory tract following inhaled Cr(0)-containing dusts (Zhitkovich, 2005).

Cr(III) creates very large, low-spin octahedral coordination complexes and chelates that are unable to easily cross the cell membrane (Cohen *et al.*, 1993) which may explain why Cr(III) is less mutagenic than Cr(VI).

Cr(III) is considered a very stable oxidation state for chromium and epidemiological studies revealed no clear association between the exposure to Cr(III) compounds and the risk of develop cancer (International Agency for Research on cancer, 1990; Agency for Toxic Substances and Disease Registry, 1993; Gibb et al. 2000; Mancuso, 1997). No effects were observed in workers exposed to Cr(III) oxide and chromic sulfide until 25 years (National Library of Medicine, 1995).

1.4.1 Chromium (VI)

Chromium (VI) is a well known carcinogen playing an important role in lung carcinoma. It is one of the studied and investigated metals concerning to mutagenicity and carcinogenicity (Kondo, K. *et al.* 2003). The International Agency for Research on Cancer (IARC) classifies Chromium (VI) belonging to Group A, group of human carcinogens (International Agency for Research on cancer, 1990). Several workers worldwide undergo an occupational exposure to Cr(VI) compounds, documented as human respiratory tract carcinogens by chronic exposure (Urbano, A. M. *et al.* 2008). These compounds can transform cells maintained in culture (Leonard, 1988; Patierno *et al.*, 1988; Elias *et al.*, 1989; Xie *et al.*, 2007; Rodrigues *et al.* 2008) and have also been reported as potent inducers of tumors in experimental animals (Rodrigues *et al.* 2008, International Agency for Research on Cancer, 1990; Landolph, 1990; Långard, 1990; Agency for Toxic Substances and Disease Registry, 1993). Tobacco smoke, chromium-containing dusts from industries, fuel combustion, portland cement, milling and concrete pavement are conditions that increase the non-occupational exposure to certain Cr(VI) compounds (Singh *et al.*, 1998; O'Brien *et al.*, 2003).

At physiological pH Cr(VI) exists in the form of chromate (CrO_4^{2-}), with a tetrahedral structure, alike to phosphate and sulfate oxyanions (Alcedo and Wetterhahn, 1990).

Cr (VI) build stable complexes with DNA, leading to mutations and breaks in DNA chain, binary and tertiary Cr-DNA bridges, interstrand Cr-DNA crosslinks, DNA-protein cross-links, simple and double DNA breaks and nitrogenous bases damages (Urbano *et al.* 2008). As soon as Cr(VI) oxyanions enter the cell, they are immediately reduced by intracellular agents to the more stable form Cr(III). The major intracellular reducers of Cr(VI) are glutathione, cysteine and ascorbate (Suzuki and Fukuda, 1990; Zhitkovich, 2005). Ascorbate rate of Cr(VI) reduction is the highest among others

reductions agents (Zhitkovich, 2005). In cases where cells are exposed to extensive exposures of Cr(VI), the mitochondrial electron transport complexes (Ryberg and Alexander, 1990), the flavoenzymes (Banks and Cooke, 1986; Mikalsen *et al*., 1989; Shi and Dalal, 1989), the hydrogen peroxide (Kawanishi *et al.*, 1986) and the hemoglobin (Fernandes *et al.* 2000) can also contribute to Cr(VI) reduction. The intracellular uptake and storage of Cr(VI) is affected by intracellular levels of reduce agents (Cohen *et al.*, 1993). The reduction of Cr(VI) by cysteine is very slow compared to other reducers and the process gives rise to transient Cr(V) and Cr(IV) species. On the other hand, the reduction by ascorbate is faster and generates Cr(IV) as the major intermediate, at physiological concentrations (Zhitkovich, 2005).

Cr(VI) in lung tissue originates respiratory distress, fibroproliferative disease, respiratory tract and pulmonary carcinomas, noncancerous tissue erosion (Glaser *et al.*, 1985; Adachi *et al.*, 1986,1987; Bright *et al.*, 1997; Singh *et al.*, 1998) and airway hypersensitivity (Bright *et al.*, 1997).

1.5 Human Bronchial Epithelial Cells

Human Bronchial Epithelial Cells were transformed by infection with SV40 virus by Curtis Harris in 1988. Colonies and morphologically altered cells were isolated and cultured and was observed that this cell lines presented an extended culture lifetime when compared to normal human bronchial epithelial cells (Reddel R.R. *et al.* 1988)

Transformation of Human Bronchial Epithelial Cells with SV40 virus gave rise to a slight increase in cell duplication times, and only a few of them (small population) rise with an unlimited proliferation potential (immortalized) (Ohnuki *et al.*, 1996).

Immortalized cell lines are used for in vitro studies since they can be manipulated by molecular biology techniques. Yet, proliferating immortalized cells may not mimic normal, terminally differentiated cells in tissues, because microenvironment play an important role and all *in vivo* conditions can´t be reproduced in *in vitro* cultures.

Also, the genetic alterations that lead these cells to grow indefinitely can modify other cell functions to. Structural features that characterize airway epithelial cells, as tight junctions, distinct basal and apical surfaces and cilia are not present in non-confluent growing cells (Veranth *et al*., 2008).

An *in vitro* study of malignant transformation of bronchial epithelial cells by Cr(VI) was already achieved in order to understand Cr(VI)-induced carcinogenesis, and an *in vitro* cellular model was established using BEAS-2B cells. This cells were exposed to 1μM Cr(VI) and changes in cell´s ploidy and a decrease in cloning efficiency was observed. (Rodrigues *et al.*, 2009).

1.6 The Warburg effect

Over the years, biochemical studies revealed that tumors presents altered metabolic profiles and high rates of glucose uptake and glycolysis. These metabolic alterations are not essential defects that lead to cancer, but may confer an advantage for most types of cancers, allowing cells invasion and survival. The genetic alterations that lead to tumors development are directly related to glycolysis, the way that cells react to hypoxia and the capacity of recruitment of new blood vessels (Dang C.V. and Semenza G.L., 1999). In hypoxia, neoplastic cells enhance glycolysis to produce anabolic precursors and energy. Ras signaling is activated in many cancers and increase glycolytic flux to lactate, regulating cancer cells metabolism (Telang *et al.*, 2007).

In 1956, Otto Heinrich Warburg, a German biochemist, measured the oxygen consumption and lactate production of cells in tumor slices, at same times. He concluded that in the presence of oxygen, glucose uptake and lactate secretion by tumor cells is higher than in normal cells (Warburg, 1956). The “Warburg effect” is been related to mutations in tumor suppressor genes, oncogenes, metabolic enzymes and in

mitochondrial DNA, reason why mitochondria is being studied and investigated concerning the metabolism of tumor cells.

1.7 Mitochondrial disfunction

Mitochondria are maternally inherited organelles present in eukaryotic cells (Henze K., 2003). Mitochondria are limited by two membranes, the inner membrane and the outer membrane. The inner mitochondrial membrane is composed by cristas, infoldings in the membrane that increase mitochondria membrane area (Lodish, 2004).

Mitochondria are the central places of ATP production in aerobic cells. Under aerobic conditions, pyruvate from glycolysis is transported into the mitochondrial matrix by active transport, being oxidated to acetyl-CoA, and enters into Krebs Cycle (figure 2)

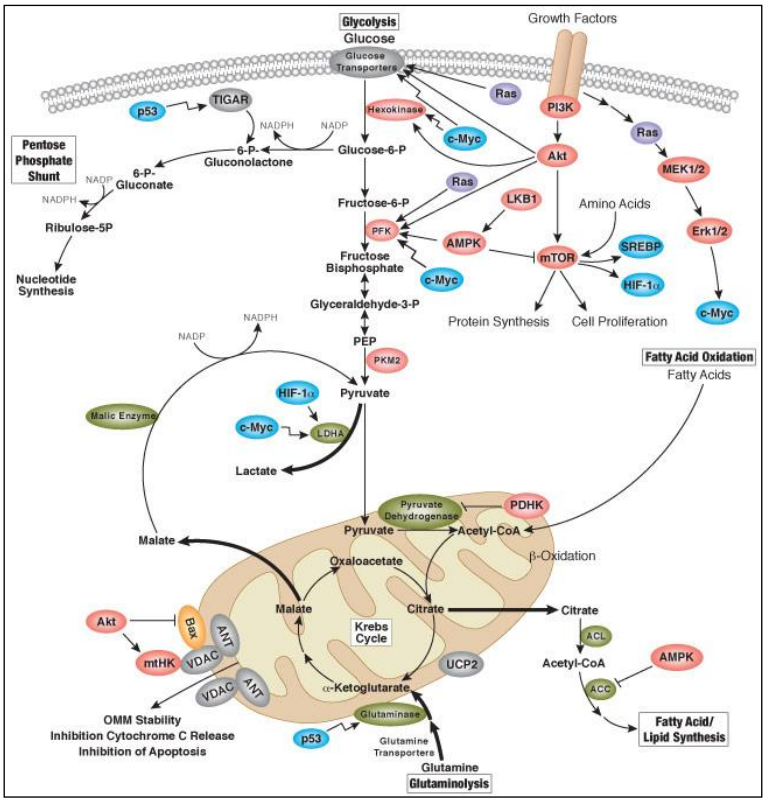

Figure 2 – Mitochondrial respiration, Krebs Cycle and the fates of pyruvate

Mitochondria play important roles in cellular energy metabolism, free radical generation, cell signaling and apoptosis. Defects in mitochondrial function have long been suspected to contribute to the development and progression of cancer. Certain malignant cells have also been reported to have alterations in mitochondrial content as compared to normal cells of the same tissue (Frezza and Gottlieb, 2009).

The morphology of mitochondria is tightly controlled by fusion and fission events in a dynamic equilibrium that determines the proper intracellular distribution of mitochondria, maintains normal mitochondrial morphology, and determines the inheritance of mtDNA. How mitochondrial DNA molecules segregate before and during mitosis determines the genetic identity of daughter cells, and is particularly relevant in several human diseases where there is heteroplasmy due to inherited or newly acquired mutations in the DNA (Wallace, 1999; Schon, 2000).There is ample evidence that the morphology of mitochondria varies by cell type (Aw and Jones, 1989; Bereiter-Hahn, 1990).

Materials and Methods

2.1 Materials

The salts used in preparation of PBS solution, *i.e.*, KCl, NaCl, KH_2PO_4 and Na_2HPO_4; the NaOH; the Bovine Serum Albumin (BSA) used in the preparation of 1% gelatin solution; the 2% type B gelatin solution and powder gelatin from bovine skin, as well as 0.25% trypsin-EDTA and 0.4% trypan blue solutions were acquired from Sigma-Aldrich Chemistry S.A. (Sintra, Portugal).

The HCl used to obtain the solution to adjust the pH was acquired from Panreac Chemistry S.A. (Barcelona, Spain).

The Fetal Bovine Serum (FBS); the LHC-9 medium; the F12 Nutrient Mixture (Ham) and the DMEM No Glucose medium, were obtained from Gibco as part of Invitrogen Life Technologies (California, USA) through Alfagene, (Lisbon, Portugal) distributor.

The Ultroser G serum substitute was obtained from PALL Life Sciences provided by Semortrade Lda. (Lisbon, Portugal).

Tetramethylrhodamine methyl ester (TMRM S68446), Calcein-acetomethoxy ester (Calcein-AM C1430), Mitotracker red, DAPI and Hoechst 33342 were purchased from Molecular Probes, Invitrogen S. A. (Barcelona, Spain).

Cox IV rabbit antibody cod. 4844 was obtained from Cell Signaling (Danvers, USA) through Izasa Lisbon distributor (Carnaxide, Lisbon).

FITC anti-rabbit, FITC mouse anti-goat and UCP2 SC-6526 were purchased to Santa Cruz Biotechnology Inc. (California, USA) through Santa Cruz Biotechnology Inc. distributor in Germany.

FIuorescein (FITC) conjugated AffiniPure F (ab') 2 Fragment Donkey anti-goat (code number 705-096-147) was obtained from Jackson ImmunoResearch Laboratories, Inc. (West Grove, PA, USA).

The 0.2 µm filters were acquired from Whatman (London, England).

The “vent-cap” canted neck non-pyrogenic and sterile flasks of 25 cm^2, 75 cm^2 and 150 cm^2; the 5 mL, 10 mL and 25 mL individually wrapped, glass disposable serological sterile pipets; the non-pyrogenic and sterile o-ring cryogenic vials of 2.0 mL and the non-pyrogenic and sterile 6 wells cell culture flasks were purchased from Corning Incorporated provided by Sigma-Aldrich Chemistry S.A. (Sintra, Portugal).

The centrifuge tubes of 15 mL and 50 mL were acquired from Orange Scientific (Braine-l'Alleud, Belgium) provided by Frilabo (Oporto, Portugal).

The microcentrifuge tubes of 1.5 mL were obtained from Bioplastics (Landgraaf, Netherlands).

All pipette tips were purchased from VWR International (Carnaxide Portugal).

The Pasteur pipettes were acquired from Normax (Marinha Grande, Portugal).

2.2 Equipment and Software

The benchtop autoclave Omega Media model was acquired from Prestige Medical (Blackburn, UK) provided by Ezequiel Panao Jorge, Electromedica (Coimbra, Portugal). The water purification system Simplicity™ was obtained from Millipore S.A. (Molsheim, France) provided by Interface, Equipamento e Tecnica Lda. (Amadora, Portugal). The Universal 32 benchtop centrifuge model was ordered from Hettich GmbH &Co. (KG, Tuttlingen, German) provided by Dias de Sousa S.A. (Oporto, Portugal). The 5417R microcentrifuge model was purchased from Eppendorf (Hamburgo, German) and provided by VWR International (Lisbon, Portugal) distributor. The pipettor ComfoPette was purchased from Orange Scientific (Braine-l’Alleud ,Belgium) provided by Frilabo (Oporto, Portugal). The 20 mL, 200 mL and 1000 mL micropipettors were acquired from Eppendorf (Hamburgo, German) and provided by

VWR International (Carnaxide Portugal). The vertical laminar flux chamber BSB3A model was acquired trough Gelaire Flow Laboratories (Australia) and provided by Interface (Amadora, Portugal). The TMS model microscope from Nikon, USA was provided by Nikon Portugal (Lisbon, Portugal). The hemocytometer was provided by Reagente 5 (Oporto, Portugal). The 3121 CO_2 incubator model from Thermo Electron Corporation was obtained through FSG (Queijas, Portugal). The CP-501 pH meter model from Elmetron (Zabrze, Poland) was acquired through Jose Manuel Gomes dos Santos, Lda. (Odivelas, Portugal). The 85135 magnetic stirrer S.N. model from VELP (New York, USA) was provided by I.L.C. (Oporto, Portugal). The 770 precision balance model from Kern (Allbstad, German) was provided by Labometer (Lisbon, Portugal); The vortex IKA vortexer set-point from Agilent Technologies (Walbronn, German) was acquired from Inopat (Oporto, Portugal). Heating plate with magnetic stirrer, model Monotherm from Variomag, Daytona Beach, Florida, USA.

The NUTSproTM NMR processing software was acquired by Acorn, Inc. (Freemont, CA, USA).

2.3 Cell lines

2.3.1 BEAS-2B cell line

The BEAS-2B cell line (Cat. No.: 95102433) was acquired to the European Collection of Cell Cultures (ECACC) in the form of a cryopreserved cellular suspension, which was then expanded and again cryopreserved in cryogenic vials. The BEAS-2B cells were derived from normal bronchial epithelium obtained in an autopsy of a non-cancerous individual. To immortalize the primary culture the cells were transfected with an adenovirus 10-SV40 hybrid virus and cloned (ECCAC-European Collection of Cells Cultures, General Cell Collection, Health Protection Agency Culture Collection, Cat.

No.: 95102433). The cells must be cultured to sub-confluence otherwise they rapidly undergo squamous terminal differentiation (ECCAC-European Collection of Cells Cultures, General Cell Collection, Health Protection Agency Culture Collection, Cat. No.: 95102433). The supplier recommends the use of a serum free bronchial epithelium growth medium (ECCAC-European Collection of Cells Cultures, General Cell Collection, Health Protection Agency Culture Collection, Cat. No.: 95102433) so the LHC-9 cell culture medium was selected. This medium is commercialized frozen in its usable form. LHC-9 medium was used to cultivate both BEAS-2B cells and CONT cell lines.

As BEAS-2B cells have anchorage-dependent growth, it is necessary to pre-coat the cell culture flasks with a matrix solution. As coating solution a 1% gelatin solution from bovine skin was selected.

2.3.2 RenG2, CONT, DRenG2 and DDRenG2 cell lines

RenG2 cell line was obtained following prolonged low-density culture of the BEAS-2B cell line in the presence of the sub-cytotoxic concentration of 1 μM hexavalent chromium [Cr(VI)], as reported by Rodrigues and collaborators (Rodrigues et al., 2009). CONT cell line was obtained following the exact same procedure but in the absence of Cr(VI).

To attain the DRenG2 cell line, 10^6 RenG2 cells were sub-cutaneously injected in nude mice and tumors were allowed to form. RenG2 cell line was established out of the resected tumors (Rodrigues et al., 2009).The DDRenG2 cell line was obtained using the same procedure but out of tumors formed in nude mice following the sub-cutaneous injection 10^6 DRenG2 cells (Rodrigues et al., 2009). CONT**,** RenG2, DRenG2 and DDRenG2 cell lines were cultured in pre-coated cell culture flasks. LHC-9

medium was used to cultivate CONT and RenG2, while Hams F12 supplemented with Ultroser was used to cultivate DRenG2 and DDRenG2 cell lines.

2.4 Methods

2.4.1 Solutions Preparation

Phosphate buffered saline solution 10x concentrated (PBS 10x)

The 10x PBS solution is a water-based salt solution containing 2.68 mM NaCL, 8.1 mM Na_2HPO_4, 2.68 mM KCl and 4.15 mM KH_2PO_4. The salts were diluted in ultrapure water and the solution pH was adjusted to 7.4. Finally, the volume was corrected to attain the desired concentration of the salts.

The 10x PBS solution was a stock solution from which, by dilution with ultrapure water, the 1x PBS solution was prepared. The 1x PBS solution was always autoclaved prior to use to guarantee its sterilization.

2 % BSA solution

The 2% BSA solution was prepared solubilizing 2.0 g of BSA in 100 mL of ultrapure water. The solution was subsequently homogenized using a magnetic stirrer and filtered under sterile conditions.

1 % Gelatin solution in PBS

The gelatin from bovine skin was acquired commercially either in the form of a 2% concentrated solution. For usage, the 2% gelatin solution was 1:1 diluted in 45 % 1x PBS and 5 % BSA 2 % solution.

Ham's F12 cell culture medium

To prepare 500 mL of F12 cell culture medium, 5 mL (1 % of the total volume) of a large spectrum antibiotic mixture containing penicillin and streptomycin and 5 mL of the serum substitute Ultroser G were diluted in 490 ml of the F12 nutrient mixture.

NaOH 1 M pH adjusting solution

This solution was obtained by dissolution of 20.0 g of NaOH in 500 mL of ultrapure water.

HCl 1 M pH adjusting solution

This solution was obtained by dissolution of 1.74 mL of HCl 37% in 98.26 mL of ultrapure water.

Ultroser G Preparation

Ultroser G is available in tablets packed in a flask of 20 mL. In order to dissolve the tablets, 20 mL of miliQ water is added to the flask, with a serological pipette or a seringe. For complete solubilization, the flask is mixed manually under continuous rotations. Each flask of 20 mL of ultroser is divided in 4 aliquots of 5 mL each. Each one of this aliquots is going to be used for the preparation of a flask of 500 mL of Ham's F12 medium, by removing 5mL of medium and adding the 5 mL of Ultroser, keeping the same volume of 500 mL of final medium.

2.4.2 Cell culture

All five cell lines (BEAS-2B, CONT, RenG2, DRenG2 and DDRenG2) were cultured in polypropylene culture flasks, previously coated with a 1 % gelatin solution (1 mL/ 25cm^2). This procedure was done at least 2 hours and up to 72 hours before flasks' use to guarantee a proper gelatin polymerization, and so, a good matrix for cells

to growth. Right before use, each flask was washed with 1x PBS after what the final volume of medium was added (5 mL/25 cm^2). BEAS-2B, CONT and RenG2 were grown in LHC-9 cell culture medium while DRenG2 and DDRenG2 were grown in Ham's F12 cell culture medium.

All the cells used throughout this study were initially cryopreserved. For this purpose Cryo Freezing Container "Mr. Frosty" was used providing the critical repeatable -1ºC/minute cooling rate required for successful cell cryopreservation and recovery.

To avoid cell death the process of thawing was done as quick as possible. Flasks were previously prepared and filled with 37 ºC pre-heated cell culture medium and the cryogenic vials were thawed at room temperature. The cell suspension was added to the flask with the help of a pipette.

All the cell lines were cultured using an initial cell density of $4x10^3/cm^2$ and when 80 % confluence was attained, cells were transferred to a new flask with new medium in a process called "*passage*". Between passages, cells where maintained in a

37 ºC and 5 % CO_2 incubator under a humidified atmosphere. On routine subculture procedures cells were harvested using a trypsin-EDTA solution (1mL/ 25cm^2). For trypsin's maximum effect, the flask containing the cells and trypsin was incubated at 37°C for half a minute. After trypsinization, 1x PBS was added to the flak (5 mL/25cm^2) to detach and collect cells. The resulting suspension was centrifuged at 1.500 rpm for 5 min and the pellets resuspended in 1 mL of growth medium until attaining a single-cell suspension. A 20 µL aliquot of this suspension was collected and used for cell counting following a 1:1 dilution with 20 µL trypan blue dye (see 2.4.2.1 section).

Whenever possible, cell aliquots were frozen in order to keep a good stock. To this end, when 80 % confluence was attained in the flaks, cells were tripsinized and counted and approximately $4x10^6$ cells were divided by each cryogenic vial. The

freezing solution used was composed of 20 % FBS and 10 % DMSO to guarantee the maintenance of cells' membrane structure and integrity and to prevent the formation of ice crystals and 70% of each cell line specific growth medium.

2.4.2.1 Cell counting procedure

As previously referred, during the procedure of cell passage cells were counted in order to attain the desired volume of cells to initiate a new flask. To this end a 1:1 single-cell suspension and trypan blue 0.2 % (v/v) solution dilution was prepared in a total volume of 40 µL. After a proper homogenization of this solution, 20 µL were collected and transferred into the hemocytometer and cells were counted.

The trypan blue solution is used to stain the dead cells once the dye quickly enters these cells as a consequence of their damaged membrane. Simultaneously, it also allows the counting of the viable cells as they do not stain blue and their cytoplasm gets brighter when surrounded by it. The number of viable cells was counted in each of the four quadrants (in blue in the figure) and the average number of viable cells per chamber was determined. To attain the final concentration of cells the medium value was multiplied by 2, the dilution factor and by 10^4, the volume of the chamber.

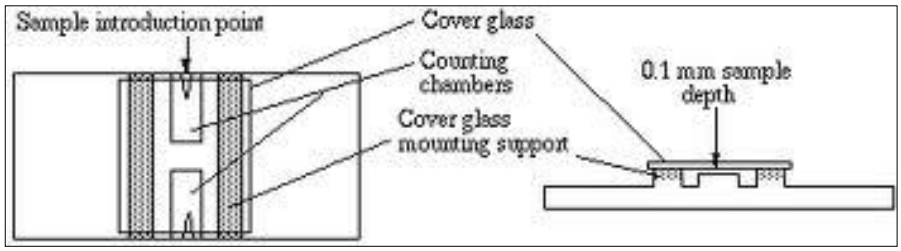

Figure 3 - Schematic representation of a hemocytometer. The suspension is pipetted into the V-shaped wells and two samples are counted for each cell line. The space below the coverslip fills through capillary action. (adapted from http://www.ruf.rice.edu/~bioslabs/methods/microscopy/cellcounting)

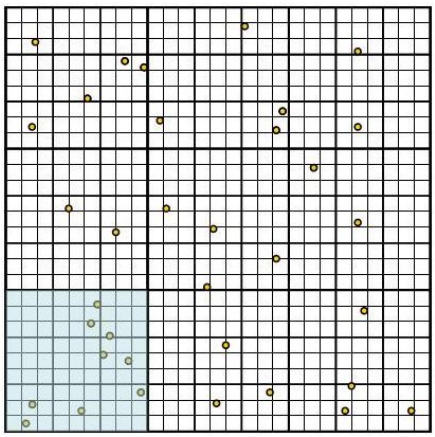

Figure 4 – Scheme of a Hemocytometer . The total number of cells per mL is obtained by multiplying the total number of living cells (not stained) found in the hemocytometer grid, in each of the 4 quadrants (area equal to the blue square in picture) by factor and 104, the volume of the chamber.

2.4.3 Mitochondria function and permeability evaluation

Mitochondria function was indirectly evaluated by observing the variations in mitochondria's membrane potential by flow cytometry using the JC-1 probe ('6,6'-tetrachloro-1,1,3,3'-tetraethylbenzimidazolcarbocyanine iodide). The protocol used is described on www.probes.invitrogen.com (see appendix). The cellular fluorescence intensity was measured using a Becton-Dickinson FACScan flow cytometer (Becton-Dickinson, San José, CA). For each analysis 10.000 events were recorded.

$1x10^{6}$ cells/mL cellular suspensions were produced in 1 mL of 1x PBS solution. From this suspension, 0.5 mL were transferred into a sterile centrifuge tube and centrifuged at 400 x g for 5 min. at room temperature. The supernatant was removed and cells were resuspended in 0.5 mL of 1x JC-1 reagent solution. Cells were allowed to incorporate the probe for 15 min at 37 °C in a 5 % CO_2 incubator. After incubation they were again centrifuged for 5 min at 400 x g and the supernatant was removed.

The pellet was finally ressuspended in 400 µL of PBS and transferred for a cytometer tube for flow cytometry analysis.

2.4.4 Live cell fluorescence microscopy

To identify the morphological features of mitochondria, a triple labeling with TMRM, Calcein-AM and Hoechst 33342 was used. TMRM is a cationic, mitochondrial selective probe that is accumulated by this organelle in a membrane potential (Δψ)-dependent manner. TMRM has been used to measure mitochondrial depolarization related to cytosolic Ca transients and to image time-dependent mitochondrial membrane potentials. Calcein-AM readily passes through the cell membrane of viable cells because of its high hydrophobicity. In the cytoplasm, calcein-AM is hydrolyzed by the cellular esterases to calcein, which remains inside the cells and emits green fluorescence. Thus, the accumulation of this probe inside the cells is indicative of membrane integrity, since damaged cell membrane in malignant cells prevents calcein from accumulating intracellularly. Hoechst 33342 dye is a cell-permeant nucleic acid stain that is selective for DNA and spectrally similar to DAPI. It is UV excitable and emits blue fluorescence when bound to DNA (maximum excitation/emission when bounded to DNA 350/461 nm). As such, Hoechst 33342 is commonly used to visualize nuclei, allowing the observation of chromatin condensation and other nuclear alterations in apoptotic cells.

4000 cells/cm^2 from each cell line (BEAS-2B, CONT, RenG2, DRenG2 and DDRenG2) were grown in 6 wells multiwell plates until 50% confluence above coverslips previously covered with gelatin. When the desired confluence was reached, growth medium was removed and 2 mL of a mixture of medium and probes (for the 12 mL of mixture it was prepared 13.56 µL TMRM, 12 µL Hoechst 33342 and 1.2 µL Calcein-AM) was added to each well. Cells were then incubated for 40 min at 37 ºC and covered with foil every time they were exposed to light. Meanwhile, 400 µL of pre-

heated to 37 ºC 1x PBS were pipetted into a chamber for fluorescent microscope studies. Coverslips were then gently removed from wells with two tweezers and the coverslip side where cells were attached was turned upside down into the chamber, allowing cells to contact with the PBS. Every split of PBS was cleaned from the sides of the chamber and the stained cells were observed under a fluorescent microscope. In case of necessity, the other coverslips on the wells could be stored in an incubator at 37 ºC.

Cellular fluorescence images were acquired with an Olympus IMT-2 inverted microscope, equipped with a xenon light source (75 watts) for epifluorescence illumination and with a 12-bit digital cooled CCD camera (Micromax, Princeton Instruments). For detection of fluorescence, 488 ± 25 nm excitation and 525 nm emission and 568 ± 25 nm excitation and 585 nm longpass emission filter settings were used for calcein and TMRM, respectively. Images were collected with exposure times ranging between 50 and 100 ms using a 40x 1.3 NA oil immersion objective (Nikon).

2.4.5 Immunofluorescence microscopy

For immunolabeling, cells were grown in 12 wells multiwell plates at a density of 4000 cells/cm^2 above coverslips previously covered with gelatin. All the five cell lines (BEAS-2B, CONT, RenG2, DRenG2 and DDRenG2) were plated at the usual initial density and grow in 2 mL of cell culture medium. When about 50% confluence was achieved, cells were incubated with Mitotraker red (125 nM) for 30 min at 37°C in the dark, as this probe is light sensitive. The multiwell was covered with foil every time it needed to be exposed to light. After incubation, the excess of Mitotraker red was removed and cells were washed once with cold 1x PBS and fixed with 2 mL of 4% paraformaldehyde during 15 min at room temperature and in dark. Paraformaldehyde was removed and cells were washed twice with PBS (1x).

The cells fixed with paraformaldehyde were permeabilized with 0.2% Triton X-100 in PBS (2 mL per well) for 5 min at room temperature, following three washes with PBST (1mL per well). PBST was then removed and cells were incubated in blocking solution (PBST supplemented with 1% non-fat powdered milk) for 30 min to one hour at 37 °C (2 mL per well), to remove non-specific staining. Cells were then incubated with a specific primary antibody (COXIV rabbit 1:200) for 24h at 37°C (200 µL per well). Each coverslip with cells was washed for 5 min in PBST supplemented with 1% non-fat powdered milk. This solution was then removed and cells were washed twice with PBST, again for 5 min each time. Cells were subsequently stained with FITC-conjugated secondary antibody (anti-rabbit for COXIV, dilution 1:100). At the end, there were 3 coverslips for each cell line, one with primary and secondary antibody, one with only secondary antibody (to test non-specific staining) and another one without antibodies (for basal fluorescence control). The three coverslips with cells were turned upside down into a microscope slide in the order referred before, using a mounting solution with DAPI and polish, to stain DNA and to fix coverslips to microscope slides, respectively. Finally, the cells were observed under a epifluorescence microscope.

Another immunolabeling assay was perform to analyze the presence of the uncoupling protein 2 in all the five cell lines (BEAS-2B, CONT, RenG2, DRenG2 and DDRenG2) with exactly the same protocol described before but with an UCP2 goat primary antibody (1:2500 dilution) and a FITC conjugated secondary anti-goat antibody.

2.4.6 Nude mice xenograft tumor experiments

Six weeks old male BALB nu/nu nude mice were subcutaneously injected in the flank using a 21-gauge needle. $10x10^6$ cells were used per each animal and 2 mice were used per each cell line. Animal experiments were carried out in accordance with the Guidelines for the Care and Use of Laboratorie Animals, directive 86/609/EEC. The

animals were weighed weekly and tumors' emergence, their width and length were also measured with calipers every week. After resection, tumors were fixed with 4% formaldehyde and the histopathological evaluation of the tumors and other resected organs (liver, kidney, heart, lung and brain) was performed.

For the determination of the tumors' histological classification, they were embedded in paraffin. 3 µm sections made and stained with hematoxylin and eosin for microscopic examination by a pathologist. Immunohistochemistry was performed for LCA (lymphoma marker; clone 2B11 + PD7/26), HMB-45 (melanosome marker), MNF116 (cytokeratin antibody marker for carcinomas; clone MNF116), and vimentin (mesenchymal marker; clone Vim 3B4). All clones were obtained from Dako Corporation (Carpinteria, CA).

2.4.7 Bioenergetic phenotype

2.4.7.1 Determination of lactate and glucose levels in the culture media

To study the bioenergetic phenotype of each cell line, the lactate production and the glucose consumption levels, as well as the tricarboxilic acid metabolites were evaluated by ^{1}H and ^{13}C NMR spectroscopy.

The lactate production and the glucose uptake levels were studied in samples collected from the cell culture medium. To this end, 4000 cells/cm^2 (initial density) were grown in 25 cm^2 culture flasks, in their specific culture medium and 200 µL of medium samples were removed at 0h, 12h, 24h and 48h and stored at -80ºC. Later on, for each sample from each cell line, a mixture of 160 µL of sample (cells and growth medium) and 40 µL of 10 mM fumarate in D_2O (99,9%) was performed. The 160 µL of sample was weighted to ensure that weight and volume differences were taken into account when concentrations of glucose consumption and lactate production were calculated.

The mixture of 160 µL of sample and 40 µL of fumarate in D_2O were put into a microcentrifuge tube and homogenized by vortex, centrifuged and finally transferred to a 3 mm NMR tube. ^1H NMR experiments were performed on a 600 MHz Varian Unity INOVA spectrometer operating at 600 MHz (14.1 Tesla). Acquisition parameters included a 30º radiofrequency observation pulse, a spectral width of 7.2 kHz and an interpulse delay of 10 seconds to allow full relaxation of all nuclei in the sample for quantification purposes. Before, Fourier transformation FIDs were multiplied by a 0.2 Hz Lorentzian to improve signal to noise ratio. Line deconvolution was made using the line-fitting routine of NUTSpro™ NMR processing software (Acorn, Inc., Freemont).

2.4.7.2 Quantification of the cell number using the trypan blue assay

The glucose and lactate levels were correlated with the number of viable in each aliquot. To this end, cells were grown in 6 wells multiwell plates, covered with 1% gelatin solution, at an initial density of 4.000 cells/cm^2, and counted at 0, 24, 48 and 72 h using the trypan blue method described before (see section 2.4.2.1). Since the number of cells in each well varies along time in culture, the volume of the aliquots containing the cellular suspension taken at 24h was 100 µL but at 48h and 72h was only 50 µL.

Statistical Analysis

The results obtained in the mitochondria membrane potential were statistically analyzed using unpaired Student's T test using GraphPad Prism software. The results represented as mean ± standard deviation (SD). Differences with $P< 0.0187$ were considered statistically significant

Results and Discussion

3. Results and Discussion

3.1 In vivo Evaluation of the Malignant Potential of the Different Cell Lines

In a previous study by our group (Rodrigues *et al*., 2009) it was demonstrated that prolonged exposure of BEAS-2B cells to a low sub-cytotoxic Cr(VI) concentration induced morphologic, cytogenetic and gene expression changes associated with the emergence of a malignant cellular phenotype. Moreover, the cells' portraying such malignant phenotype, RenG2, when injected in nude mice induced tumors (Rodrigues *et al*., 2010). Out of the tumor it was possible to establish a new cell line named DRenG2, which also induced tumors in nude mice. Out of DRenG2-induced tumor it was established another cell line (DDRenG2) (Rodrigues *et al*., 2010).

Attempting to compare the malignant potential of RenG2, DRenG2 and DDRenG2 cell lines, preliminary studies were performed injecting 10^7 million cells of each cell line in BALCc /nude mice. As illustrated in Figure 5, mice subcutaneously (s.c) injected with DDRenG2 developed tumors quickly within three weeks, while DRenG2 injected mice only developed tumors four weeks later, one week later than the DDRenG2. RenG2 injected mice developed tumors within two months while no tumors were observed with either BEAS-2B cells or control cells as reported earlier (Rodrigues *et al*., 2009). These preliminary results suggested that DDRenG2 are more malignant than DRenG2 and the less malignant cell line is RenG2. Thus, it appears that the malignant potential of the cell lines can be increased by contact with nude mice stroma.

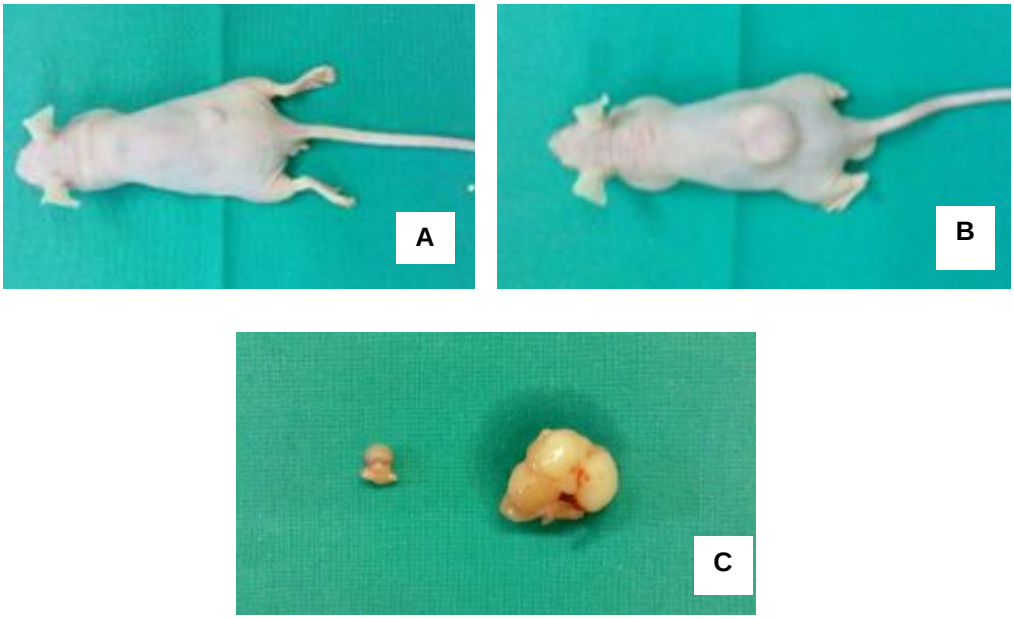

Figure 5 - Tumors induced in BALB/c-nude mice injected with DRenG2 cell line (**A**) and DDRenG2 cell line (**B**), tumors after extraction (**C**). DRenG2 tumor had 10x8 mm diameter and DDRenG2 tumor had 12x15 mm diameter. Immunohistological analysis of the tumors induced upon s.c. injection into nude mice revealed their human epithelial origin.

3.2 Mitochondria Function

3.2.1 Mitochondrial Potential Evaluation

Mitochondria are central to cell metabolism and energy production and oncogenic *RAS* expression has been reported to induce an increase in mitochondrial mass and mitochondrial DNA, as well as to mitochondrial superoxide generation. With time, these mitochondrial changes evolved into a severe mitochondrial dysfunction characterized by the accumulation of depolarized mitochondria around the cells' nucleus (Moiseeva O., *et al.* 2009). With that in mind, it was decided to evaluate the membrane potential ($\Delta\psi m$) of the two non-malignant bronchial epithelial cell lines (BEAS-2B and CONT) and of the three malignant cell lines (RenG2, DRenG2 and DDRenG2), using the

cationic fluorescent probe 5,5',6,6'-tetrachloro-1,1',3,3'-tetraethyl benzimidazolcarbocyanine iodide (JC-1). JC-1 which localizes to normal mitochondrial membranes as red aggregates and turns into a green monomer upon membrane depolarization. As illustrated in Table I flow cytometry analysis revealed that the ratio of red/green mitochondria was significantly decreased in the malignant cell lines RenG2, DRenG2 and DDRenG2, thus confirming that more malignant cells have relative to BEAS-2B progenitor cells a statistically significant increase in depolarized mitochondria. Conversely, the non-malignant CONT portrayed an opposite behavior with a statistically significant increase in polarized mitochondria in relation to BEAS-2B cells.

Table I – Different cell lines $\Delta\psi m$ evaluated by flow cytometry using the JC-1 dye

BEAS-2B	CONT	RenG2	DRenG2	DDRenG2
R =1.4 ± 0.17	R= 2.0 ± 0.26*	R= 0.93 ± 0.24**	R= 0.38 ± 0.1***	R= 0.42 ± 0.1****

Cells were seeded at a 4000 cell/cm2 and grown to 80% confluence. 5 x 10^5 cells were treated as described in Materials and Methods to evaluate membrane potential. The ratio of aggregates to monomers was calculated by measuring the red to green fluorescence. The results represent the mean ± SD of at least three independent experiments carried out in triplicate. *P< 0.0029; **P< 0.0187; ***P< 0.0009; ****P< 0.001 when compared with BEAS-2B cells. Student's T test was used.

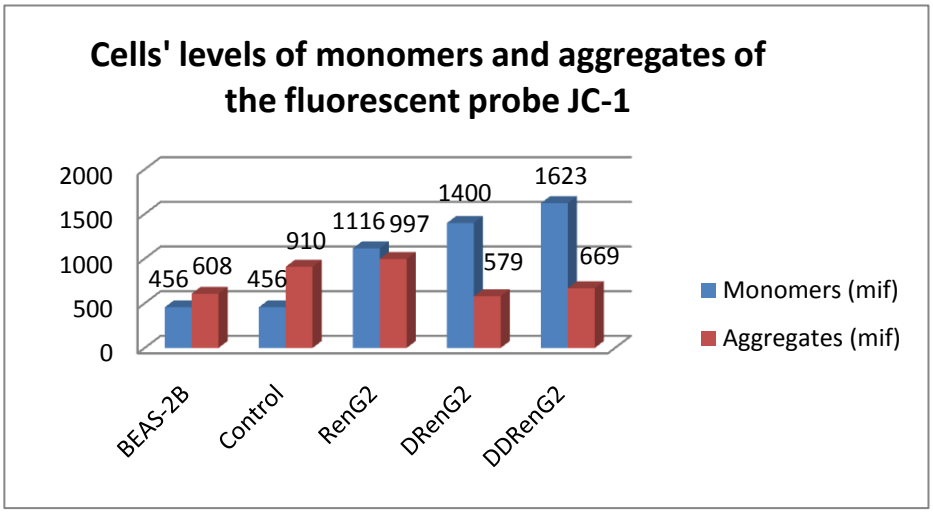

Figure 6 – Representative experiment revealing that more malignant cell lines have a higher proportion of depolarized mitochondria. Experiments were carried out as described in Materials and Methods and values represent the mean red (aggregates) to mean green (monomers) fluorescence values obtained by flow cytometry using a Bencton Dickinson FACScalibur.

3.2.2 Mitochondria Morphology Evaluation

It is known that mitochondria respond rapidly to cell injury and that response often includes unusual morphologies, i.e., donut-shaped mitochondria, absence of the typical branched structures and, occasionally, mitochondrial aggregates (De Vos *et al*., 1998; Funk *et al.*, 1999). Examples of altered mitochondria are observed in cells with defective oxidative phosphorylation such as Rho-0 cells, and cells undergoing apoptosis due to staurosporin treatment. Cell cycle dependent-changes in mitochondria morphology were reported in osteosarcoma cells (Margineantu D.H., *et al.* 2002) G1 phase cells presenting mostly a reticular mitochondria, possibly, because their metabolism is focused on energy production and protein and lipid synthesis, while cells in S phase have fragmented and perinuclear mitochondria (Barni S., *et al.* 1996; Van den Bogert *et al.*, 1988**;** Leprat P. *et al.* 1990; Karbowski M., *et al* 2001; Margineantu D.H., *et al.* 2002).

Thus, having in mind that altered mitochondria polarization corresponds to altered cellular metabolism which, possibly, correlates with altered mitochondria morphology and cellular localization; it was decided to evaluate by fluorescence microscopy these two features in all the five cell lines. To this end, the probes TMRM, Hoechst 33342 and calcein were used to evaluate in live cells the mitochondria structure, DNA and cells' viability respectively. The images represented in Figures 7.1-7.5, revealed that differences in mitochondria morphology and biogenesis are remarkable between the non malignant cell lines and the more malignant derivative cell lines DRenG2 and DDRenG2. In BEAS-2B and CONT mitochondria perinuclear localization was quite clear (Figures 7.1 and 7.2) while in DDRenG2 the plasma membrane protrusion of thin filopodia for cellular detachment, triggered the clustering of mitochondria towards the cell nuclei and forming an extensive mitochondria network (Figure 7.5).

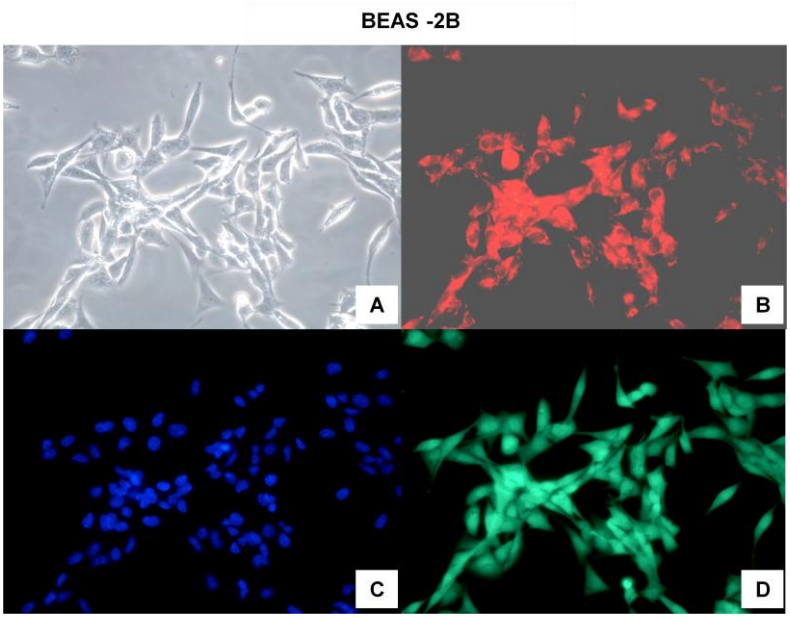

Figure 7.1 – Fluorescence microscopy images of BEAS-2B cells. **A -** cells with no probes; **B** - TMRM; **C** - Calcein; **D** – Hoechst. Cells' were cultured and treated with probles as described in Materials and Methods

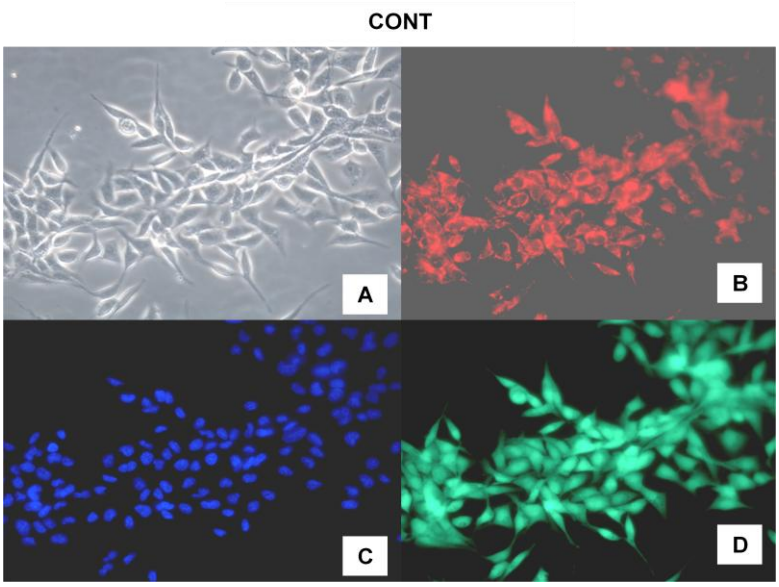

Figura 7.2 - Fluorescence microscopy images of CONT cells. **A -** cells with no probes; **B** - TMRM; **C** - Calcein; **D** – Hoechst. Cells' were cultured and treated with probles as described in Materials and Methods

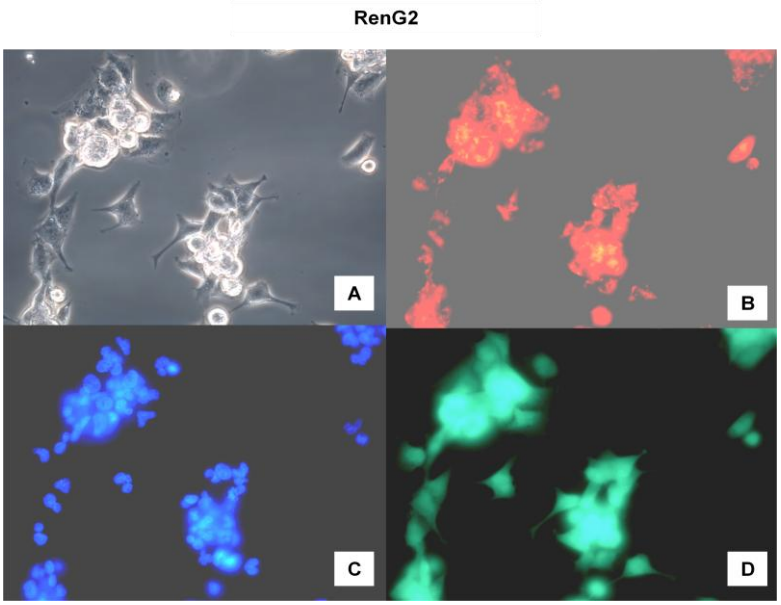

Figura 7.3 - Fluorescence microscopy images of RenG2 cells **A -** cells with no probes; **B** - TMRM ; **C** - Calcein; **D** – Hoechst. Cells' were cultured and treated with probles as described in Materials and Methods

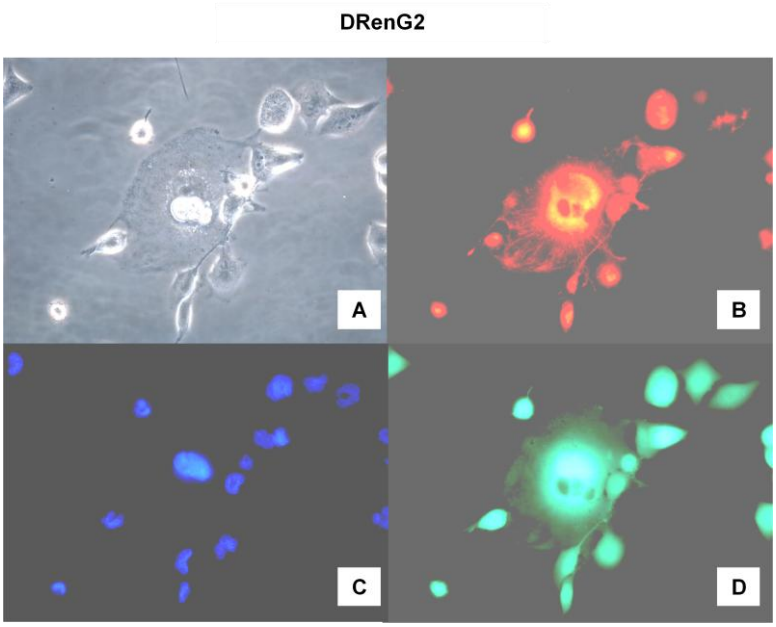

Figura 7.4 - Fluorescence microscopy images of DRenG2 cells. **A -** cells with no probes; **B** - TMRM; **C** - Calcein; **D** – Hoechst. Cells' were cultured and treated with probes as described in Materials and Methods

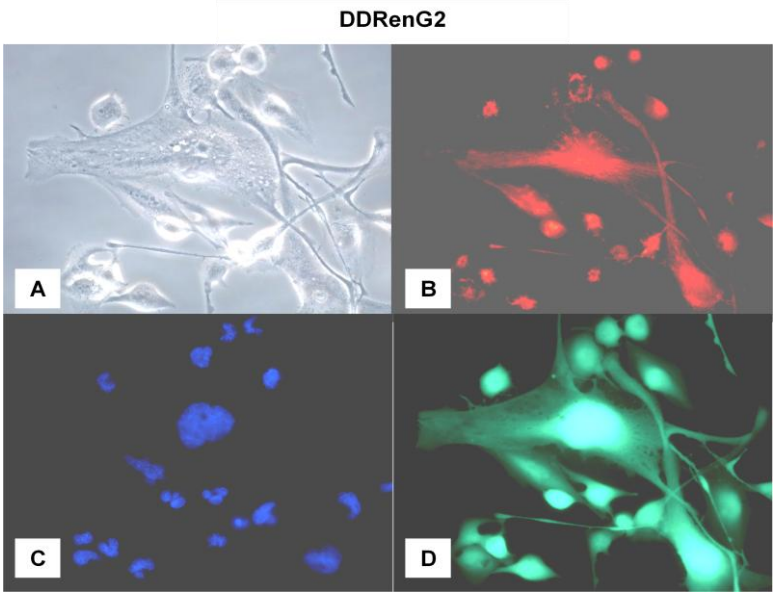

Figura 7.5 - Fluorescence microscopy images of DDRenG2 cells. **A -** cells with no probes; **B** - TMRM; **C** - Calcein; **D** – Hoechst. Cells' were cultured and treated with probles as described in Materials and Methods

The low ∆ψm values obtained for the more malignant cell lines, suggestive that cells have very low mitotic potential, as high ∆ψm values are required for the G2/M phase of the cell cycle to occur (Martínez-Diez *et al*., 2006) may also explain the mitochondria cellular localization in the more malignant cells, particularly DReng2 and DDRenG2. In fact, in actively dividing cells, during the early stages of mitosis, mitochondria are excluded from the cellular space, where the mitotic spindle is being assembled (prophase), as well as from the equator of the spindle where the chromosomes line up (metaphase) (Martínez-Diez *et al*., 2006). In contrast, particularly in DDRenG2 malignant cell line is possible to observe that mitochondria are involving all the cellular space including the nuclear (Figure 7.5).

3.2. 3. Evaluation of Cox(IV) and UCP2 Expression

The immunocytochemistry assay using the primary antibody Cox (IV) for rabbit and the second antibody FITC anti-rabbit show inespecific staining. Concerning UCP2 antibody for goat using FITC anti-goat as secondary antibody, the same results were obtained. Observing coverslips at fluorescence microscope, there was a particularly good imaging stain for DAPI and Mitotracker Red, but inespecific staining for the antibody. Probably the dilution prepared for the primary antibody wasn`t the most indicated, and this experiences must be repeated for adjusting the antibody`s ideal dilution factor. With UCP2 antibody, the dilution prepared was 1:2500, good for Western Blot, but not for immunocytochemistry assay. The dilution that should be used was 1:100 or 1:200. This part of the project must be repeated for improving the protocol and adjust the dilutions or even the antibodies and the pair of antibodies to use.

3.3 Cells' Bioenergetic Phenotype

Altered cellular metabolism is a hallmark of tumorigenesis. The increased glucose capture of tumor cells could result from an augmented demand for carbon skeletons, to sustain uncontrolled proliferation, and/or from a shift in the pathway used for energy provision during cellular proliferation. The latter was suggested by Otto Warburg many years ago (Warburg O. 1956) but remained largely unexplored until the recent renaissance of the so-called "Warburg effect" in cancer biology (Garber K., 2006). Moreover, on their way to a more malignant phenotype, cancer cells undergo complete metabolic reprogramming to attain nutrient self-sufficiency for proliferation and survival (Weinberg, 2011).

Since the results obtained suggested that the more malignant cells lines have mitochondrial dysfunction, potentially coupled with changes in organelle bioenergetics, it was decided to evaluate the cells' glycolytic flux. In order to access lactate production and glucose consumption ^{1}H NMR spectroscopy was used to access lactate and glucose levels in growth media, at different time points, along the cultivation process of the different cell lines. Figure 7.6 illustrates two superimposed ^{1}H NMR spectra of BEAS-2B cells and of the malignant derivative DRenG2 at different time points along cultivation. Clear differences in lactate production are beginning to emerge just 12 hours after the cells' being plated, and were rather different 24 hours later. As a matter of fact, the remarkable increase in lactate production by DRenG2 contrasts with apparent similar glucose levels between the two cell lines. As revealed, the more malignant DRenG2 has a much more pronounced glycolytic phenotype than non-malignant BEAS-2B cells, which correlates with DRenG2 lower $\Delta\psi m$ value.

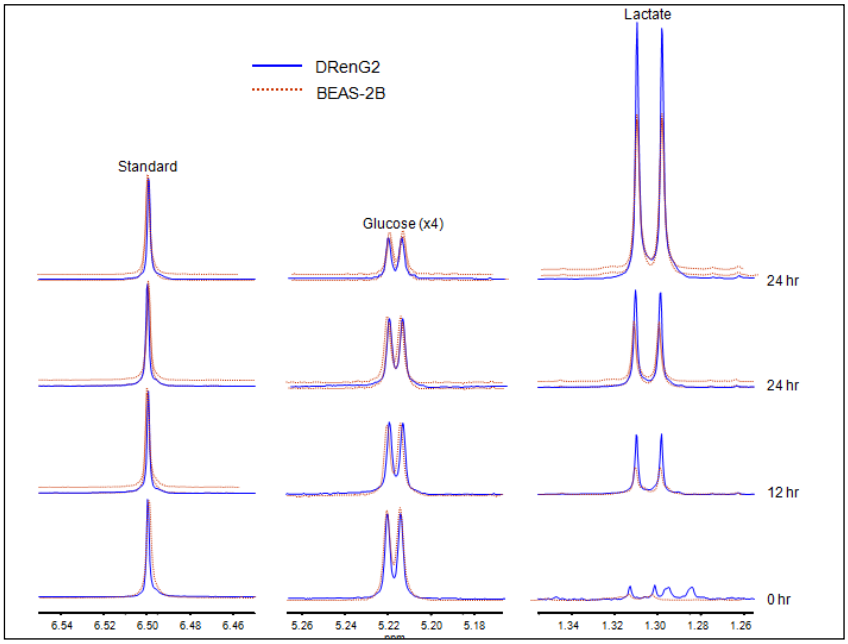

Figure 7.6 - 600 MHz representative 1^{H} NMR spectra of BEAS-2B and DRenG2 cell lines. Expansion of the of the glucose C1 proton doublet at 5.22 ppm and of the lactate C2 proton doublet at 1.33 ppm. The Standard corresponds to Fumarate at 6.5 ppm. Cells' culture conditions and aliquots collection, as well as spectra acquisition was performed as described in Materials and Methods.

As illustrated, increasing malignancy corresponds to a more pronounced glycolytic phenotype. However, the DRenG2 and DDRenG2 shift to a more glycolytic phenotype cannot only be explained on the basis that progression through the cell cycle is supported by nonrespiratory modes of energy generation, as a result of the inhibition of mitochondrial function by cyclin D1 (Sakamaki T., *et al*. 2006). In fact, the malignant DRenG2 and DDRenG2 slowly divide when compared with RenG2 or CONT (Figure 7.8). Thus, the shift to a more glycolytic phenotype may also be due to a direct effect of hypoxia-inducible factor 1α on mitochondrial bioenergetics (Kim J.W., *et al.* 2006); mutations in oncogenes and proteins related to signal transduction pathways (MYC, Akt, and mTOR) that, in turn, promote changes in the expression of genes involved in cellular energetic metabolism (Osthus R.C., *et al*. 2000) or directly interfere with mitochondrial bioenergetics by affecting the biogenesis of specific respiratory complexes (Matoba S., *et al.* 2006); and finally by mutations in mitochondrial DNA

(Polyak K., *et al.* 1998) or in nuclear genes involved in the metabolic and bioenergetic function of the organelle (Baysal B.E., *et al.* 2000).

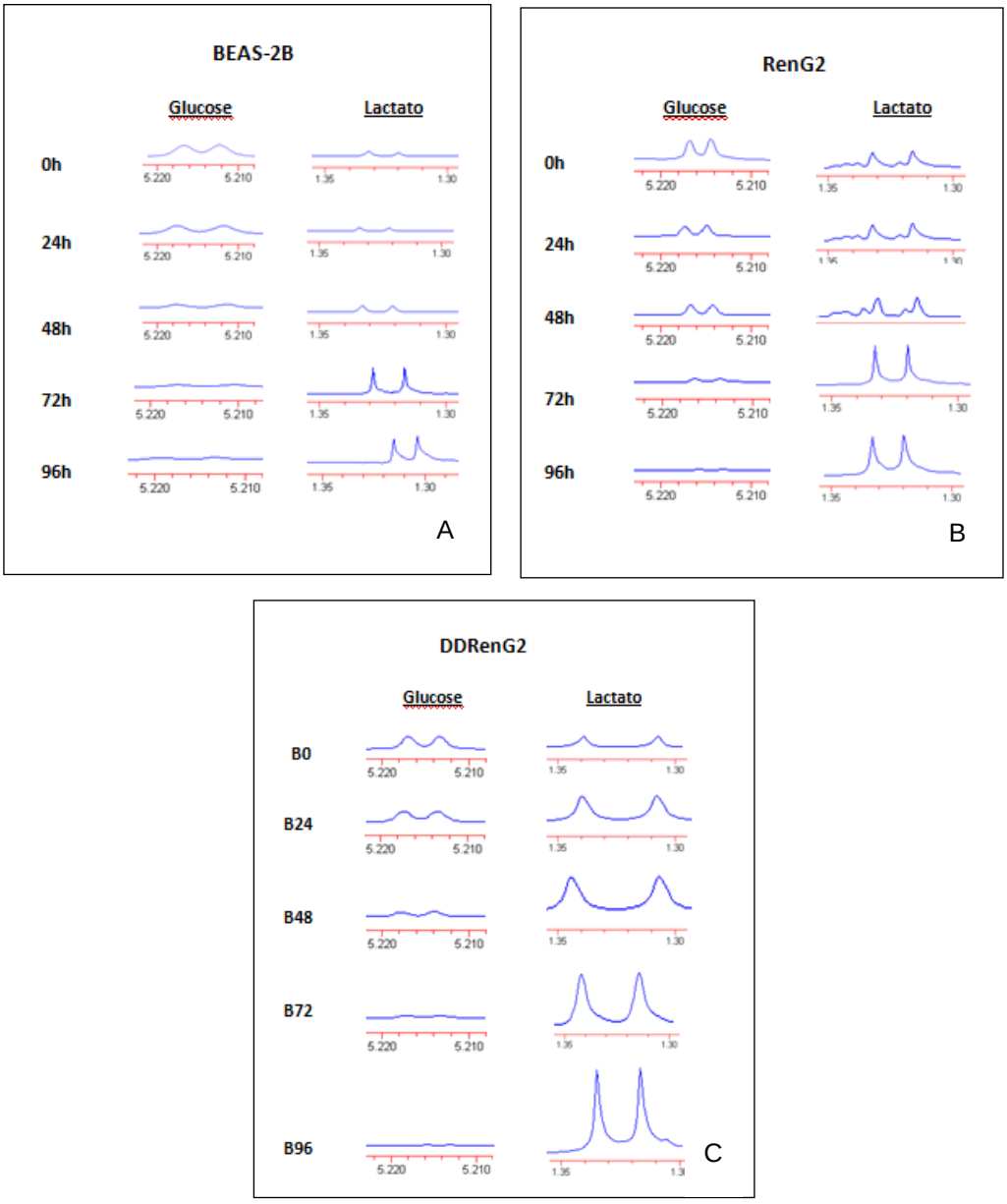

Figure 7.7 – Glucose consumption and lactate production evaluated by 1H NMR spectroscopy. A- BEAS-2B cell line,; B-RenG2; C- DDRenG2.

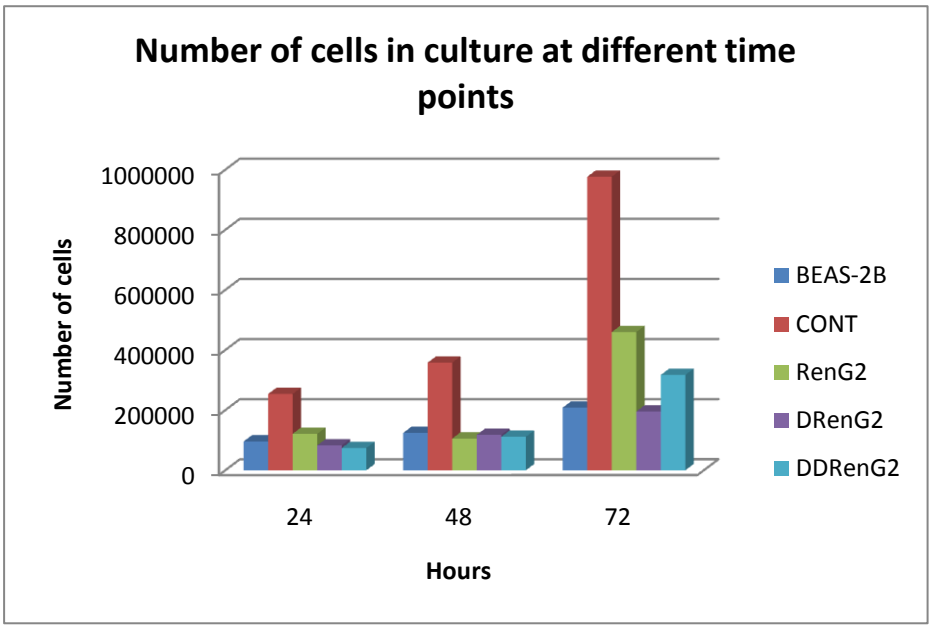

Figure 7.8 – Quantification of cell number at 24h, 48h and 72h using the trypan blue assay as described in Materials and Methods.

Control cell line (CONT) is the most replicative cell line followed by RenG2 cell line and DDRenG2 cell line. The major differences observed in cell growth are between 48h and 72h. At this time points cells are probably in exponential growth and so, the increase in glucose consumptions are from 48h and further. The rates of Lactate secretion also tend to increase, compared with figures 7.6 and 7.7. The shift of glycolic rate is almost certainly related with the set points of proliferation of cell lines.

Conclusions

Conclusions

In this study we confirmed previous evidence that the progression towards a more malignant phenotype involves metabolic reprogramming to a more glycolytic phenotype even in malignant cells that are quickly dividing. This metabolic reprogramming involved mitochondria depolarization and morphological changes. Therefore, more detailed information regarding the mechanism(s) involved in this metabolic shift should be addressed in the future.

Mitochondria generate energy through oxidative phosphorylation, which transfers electrons from NADH to O_2 molecules and leads to ATP synthesis. To further evaluate the mitochondrial contribution to the energy metabolism of the different cell lines new immunocytochemistry assay must be performed.

References

References

1. Adachi S., Yoshimura H, Katayama H, and Takemoto K (1986) “Effects of chromium compounds on the respiratory system. IV. Long-term inhalation of chromic acid mist in electroplating to ICR female mice” *Sangyo Igaku.* **28**:283-287.

2. Adachi S (1987) “Effects of chromium compounds on the respiratory system. V. Long-term inhalation of chromic acid mist in electroplating by C57BL female mice and recapitulation of our experimental studies.” *Sangyo Igaku.* **29**:17-33.

3. Agency for Toxic Substances and Disease Registry (1993) “Toxicological Profile for Chromium”, U.S. Department of Health and Human Services, Washington DC, USA.

4. Alcedo J.A., and Wetterhahn K.E. (1990). “Chromium toxicity and carcinogenesis” *Int. Rev. Exp. Pathol.* **31**:85-108.

5. Aw, T.Y., Jones, D.P., (1989). “Nutient suply and mitochondrial function.” *Annu. Rev. Nutr.* **9**:229-251.

6. Baysal BE, Ferrell RE, Willett-Brozick JE, et al. (2000). “Mutations in SDHD, a mitochondrial complex II gene, in hereditary paraganglioma.” *Science.* **287**:848–51.

7. Banks R. B., and Cooke R.T. Jr. (1986) “Chromate reduction by rabbit liver aldehyde oxidase”. *Biochem Biophys Res Commun.* **137**:8-14.

8. Barni, S., Sciola, L., Spano, A., Pippia, P.(1996). “Static cytofluorometry and fluorescence morphology of mitochondria and DNA in proliferating fibroblasts.” *Biotech*. Histochem. **71**:66–70.

9. Bereiter-Hahn, J.(1990). “Behavior of mitochondria in the living cell.” *Int. Rev. Cytol.* **122**:1-63.

10. Bright P, Burge PS, O’Hickey SP, Gannon PF, Robertson AS, and Boran A (1997) “Occupational asthma due to chrome and nickel electroplating.” *Thorax.* **52**:28-32.

11. Chiang AC, Massagué J (2008). "Molecular basis of metastasis". *The New England Journal of Medicine.* **359**:2814–23

12. Cohen M. D., Kargacin B., Klein C.B., and Costa M. (1993). “Mechanisms of chromium carcinogenicity”. *Crit. Rev.Toxicol.* **23**:255-281.

13. Ding M. and Shi X. (2000) “Molecular mechanisms of Cr(VI)-induced carcinogenesis”. *Mol Cell Biochem* 293-300.

14. Elias Z., Poirot O., Pezerat H., Suquet H., Schneider O., Daniere M.C., Terzetti F., Baruthio F., Fournier M., and Cavelier C. (1989). “Cytotoxic and neoplastic transforming effects of industrial hexavalent chromium pigments in Syrian hamster embryo cells” *Carcinogenesis* **10**: 2043-2052.

15. Frezza C., Gottlieb E. (2009). “Mitochondria in cancer: not just innocent bystanders”. *Semin Cancer Biol*. **19**:4-11.

16. Garber K. (2006).“Energy deregulation: licensing tumors to grow.” *Science*. **312**: 1158-9.

17. Gatenby R. A., Gillies R.J. (2004). “Why do cancers have high aerobic glycolysis?” *Nat Rev cancer* **4**:891-9.

18. Gibb H.J., Lees PS, Pinsky PF, Rooneym BC. (2000). “Lung cancer among workers in chromium chemical production.” *Am. J. Ind. Med.* **38**:115–126.

19. Glaser U., Hocharainer D., Kloppel H., and Kuhnen H. (1985). “Low level chromium (VI) inhalation effects on alveolar macrophages and immune functions in Wistar rats.” *Arch Toxicol*. **57**: 250-256.

20. Hanahan D., Weinberg R.A. (2000). “The Hallmarks of cancer”. *Cell* **100**:57-70.

21. Hanahan D., Weinberg R.A. (2011). “The Hallmarks of cancer: The Next Generation”. *Cell* **144**:647-674.

22. Haton A.; Jean, Hopkins Susan, Johnson Charles William, McLaughlin Maryanna Quon Warner David, LaHart Wright, Jill D. (2009). “Human Biology and Health.” Englewood Cliffs: Prentice Hall. pp. 108–118

23. Henze K., and Martin W. (2003). "Evolutionary biology: essence of mitochondria". *Nature* **426**:127–8.

24. International Agency for Research on Cancer (1990) “Chromium, nikel and welding. IARC Monographs on the Evaluation of Carcinogenic Risks to Humans” **49**:49-256, World Health Organization, Lyon, France.

25. Kawanishi S., Inoue S., and Sano S. (1986) “Mechanism of DNA cleavage induced by sodium chromate (VI) in the presence of hydrogen peroxide”. *J. Biol. Chem.* **261**:5952-5958.

26. Karbowski, M., Spodnik, J.H., Teranishi, M., et al. (2001). “Opposite effects of microtubule-stabilizing and microtubule-destabilizing drugs on biogenesis of mitochondria in mammalian cells.” *J. Cell Sci.* **114**:281–291.

27. Kondo K, Takahashi Y, Ishikawa S, Uchihara H, Hirose Y, Yoshizawa K, Tsuyuguchi M, Takizawa H, Miyoshi T, Sakiyama S, Monden Y. (2003). “Microscopic analysis of chromium accumulation in the bronchi and lung of chromate workers.” *Cancer* **98**:2420–2429.

28. Landolph J.R. (1990). “Neoplastic transformation of mammalian cells by carcinogenic metal compound: cellular and molecular mechanisms. In: Foulkes EC eds.” *Biological Effects of Heavy Metals*. Florida, CRC Press **2**:1-18.

29. Långard S. (1990). “One hundred years of chromium and cancer: a review of epidemiological evidence and selected case reports.” *Am. J. Ind. Med* **17**:189–215.

30. Leprat, P., Ratinaud, M.H., Maftah, A., Petit, J.M., Julien, R.(1990). “Use of nonyl acridine orange and rhodamine 123 to follow biosynthesis and functional assembly of mitochondrial during L1210 cell cycle.” *Exp. Cell Res.* **186**:130–137

31. Leonard A. (1988). “Mechanisms in metal genotoxicity: significance of in vitro approaches”. *Mutat. Res.* **198**:321-326.

32. Lodish H.B., Arnold; Matsudaira, Paul; Kaiser, Chris A.; Krieger, Monty; Scott, Matthew P.; Zipursky, Lawrence and Darnell, James (2004).”Molecular Cell Biology”, 5th edition. Freeman. USA.

33. Funk, R.H., Nagel, F., Wonka, F., Krinke, H.E., Golfert, F., Hofer, A. (1999). “Effects of heat shock on the functional morphology of cell organelles observed by video – enhanced microscopy.” **255**:458-465

34. Kim JW, Dang CV.(2006). “Cancer's molecular sweet tooth and the Warburg effect.” *Cancer Res*. **66**:8927–30.

35. Mancuso TF. (1997). “Chromium as an industrial carcinogen: Part I.” *Am. J. Ind. Med.* **31**:1291–39.

36. Margineantu DH, Gregory Cox W, Sundell L, Sherwood SW, Beechem JM, Capaldi RA.(2002).“Cell cycle dependent morphology changes and associated mitochondrial DNA redistribution in mitochondria of human cell lines.” *Mitochondrion*.**1**:425-435

37. Martinez-Dias M, Santamaria G, Ortega AD, Cuezva JM. (2006).“Bopgemesos and Dynamics of mitochondria during the cell cycle: Significance of 3’UTRs”.*PLoS One.***20**:1:e107

38. Matoba S, Kang JG, Patino WD, et al.(2006). “p53 regulates mitochondrial respiration.” *Science*. **312**:1650–3

39. Mikalsen A., Alexander J., and Ryberg D. (1989). “Microsomal metabolism of hexavalent chromium. Inhibitory effect of oxygen and involvement of cytochrome P-450.” *Chem Biol Interact.* **69**:175-192.

40. Moiseeva O, Bourdeau V, Roux A, Deschênes-Simard X, Ferbeyre G. (2009). “Mitochondrial dysfunction contributes to oncogene-induced senescence.” *Mol Cell Biol.* **16**:4495-4507.

41. National Library of Medicine (1995). “Hazardous substances data bank: Chromium (III) acetate, chromium (III) oxide”, Bethesda, MD.

42. O’Brien T.J., Ceryak S., Patierno S.R. (2003). “Complexities of chromium carcinogenesis: role of cellular response, repair and recovery mechanisms”. *Mutat. Res.* **533**:3-36.

43. Ohnuki Y., Reddel R.R., Bates S.E., Lehman T.A., Lechner J.F. and Harris C.C. (1996). “Chromosomal Changes and Progressive Tumorigenesis of Human Bronchial Epithelial Cell Lines”. *Cancer Genet. Cytogenet.* **92**:99 -110.

44. Osthus RC, Shim H, Kim S, et al. (2006). “Deregulation of glucose transporter 1 and glycolytic gene expression by c-Myc.” *J Biol Chem.* **275**:21797–800.

45. Patierno S.R., Banh D., and Landolph J.R. (1988). “Transformation of C3H/1OT1/2 mouse embryo cells to focus formation and anchorage independence by insoluble lead chromate but not soluble calcium chromate: relationship to mutagenesis and internalization of lead chromate particles”. *Cancer Res*. **48**:5280-5288.

46. Polyak K, Li Y, Zhu H, et al. (1998). “Somatic mutations of the mitochondrial genome in human colorectal tumours.” *Nat Genet.* **20**: 291–3.

47. Reddel R.R., Ke Y., Gerwin B.I., McMenamin M.G., Lechner J.F., Su R.T., Brash D.E., Park J-B., Rhim J.S. and Harris C.C. (1988). “Transformation of Human

Bronchial Epithelial cells by Infection with SV40 or Adenovirus-12 SV40 Hybrid Virus, or Transfection via Strontium Phosphate Coprecipitation with a Plasmid Containing SV40 Early Region Genes". *Cancer Research.* **48**:1904-1909.

48. Ryberg D., and Alexander J. (1990). "Mechanisms of chromium toxicity in mitochondria". *Chem Biol Interact.* **75**:141-151.

49. Rodrigues C.F., Urbano. A.M., Matoso E., Carreira I., Almeida A., Santos P., Botelho F., Carvalho L., Alves M., Monteiro C., Costa A.N., Moreno V., Alpoim M.C. (2008). "Human bronchial epithelial cells malignantly transformed by hexavalent chromium exhibit an aneuploid phenotype but no microsatellite instability". *Mutation Research.* **670**: 42-52.

50. Rodrigues C.F.D., Almeida A., Carreira I.M., Matoso E.,. Urbano A.M, Botelho M.F., Carvalho L., Alves M., Monteiro C. and Alpoim M.C. (2009). "Hexavalent chromium and lung cancer: new perspectives!" *The FEBS J.* **276**: 339.

51. Sakamaki T, Casimiro MC, Ju X, Quong AA, Katiyar S, Liu M, Jiao X, Li A, Zhang X, Lu Y, Wang C, Byers S, Nicholson R, Link T, Shemluck M, Yang J, Fricke ST, Novikoff PM, Papanikolaou A, Arnold A, Albanese C, Pestell R. (2006). "Cyclin d1 determines mitochondrial function in vivo." *Mol Cell Biol.* **26**:5449–69.

52. Shi X. L., and Dalal N.S. (1989). "Chromium (V) and hydroxyl radical formation during glutathione reductase-catalyzed reduction of chromium (VI)". *Biochem Biophys Res. Commun.* **163**:627-634.

53. Singh J., Carlisle D.L., Pritvhard D.E. and Patierno S.R. (1998). "Chromium-induced genotoxicity and apoptosis: relationship to chromium carcinogenesis (review)." *Oncol Rep***. 5**:1307-1318.

54. Suzuki Y, Fukuda K. (1990). “Reduction of hexavalent chromium by ascorbic acid and glutathione with special reference to the rat lung.” *Arch. Toxicol.* **64**:169–176.

55. Telang S., Lane A. N., Nelson K.K., Arumugam S., Chesney J. (2007). “The oncoprotein H-Ras ^{v12} increases mitochondrial metabolism”. *Molecular Cancer.* **6**:77.

56. Thun M.J., Hannan L.M., Adams-Campbell L.L. *et al*. (2008). "Lung Cancer Occurrence in Never-Smokers: An Analysis of 13 Cohorts and 22 Cancer Registry Studies". *PLoS Medicine.***5**:185.

57. Tomashefski J.F., Cagle P.T. Farver C.F. & A.E. Fraire (2008). “Dail and Hammar`s Pulmonary Pathology. Volume II. 3th Edition.” Springer.

58. Tyczynski J.E., Bray F. & Parkin D. M.(2003) “Lung Cancer in Europe in 2000: epidemiology, prevention and early detection.” *The lancet oncology*.**4**:45-55.

59. Urbano A.M., Rodrigues C.F.D., Alpoim M.C. (2008). “Hexavalent chromium exposure, genomic instability and lung cancer”. *Gene Ther. Mol. Biol.***12**:219-238.

60. Van den Bogert, C., Muus, P., Haanen, C., Pennings, A., Metils, T.E. & Kroon, A.M. (1988). “Mitochondrial biogenesis and mictochondrial activity during the progression of the cell cycle of human leukaemick cell.” *Exp. Cell Res*.**179**:143.

61. Veranth J.M., Cutler N.S., Kaser E.G., Reilly C.A., Yost G.S. (2008). “Effects of cell type and culture media on Interleukin-6 secretion in response to environmental particles”. *Toxicology in Vitro.* **22**:498-509.

62. www.virtualmedicalcentre.com

63. Wallace D.C. (1999). “Mitochondrial disease in men and mouse.” *Science.* **283**: 1482-1488.

64. Warburg O.(1956). “On respiratory impairment in cancer cells.” *Science*. **124**:269-70.

65. Warburg O. (1956). “On the origin of cancer cells”. *Science*. **123**:309-14.

66. (WHO. 2010).

67. Whittemore, S. (2004). “The Respiratory System.” Chelsea House Publishers, New York.

68. Wistuba I.I. & A.F. Gazdar (2006). “Lung cancer preneoplasia.” *The Annual Review of Pathology.* **1**:331-48. Schon, E. A. (2000). “Mitochondrial genetics and disease.” *Trends Biochem*. Sci. **25**:555-560.

69. Xie H., Holmes A.L., Wise S.S., Huang S., Peng C. and Wise J.P.Sr. (2007). “Neoplastic transformation of human bronchial cells by lead chromate particles”. *Am. J. Respir. Cell. Mol. Biol.* **37**:544-552.

70. Yeung S.J., Pan J., Lee M.H. (2008). “Roles of p53, MYC and HIF-1 in regulating glycolysis – the seventh hallmark of cancer”. *Cell Mol Life Sci.* **65**: 3981-99.

71. Zhitkovich, A. “Chromium: exposure, toxicity and biomonitoring approaches. In: Wilson, SH.; Suk, WA., editors. Biomarkers of Environmentally Associated

Disease: Technologies, Concepts, and Perspectives. CRC Press LLC; New York: 2002. p. 269-287.

72. Zhitkovich A. (2005). “Importance of chromium-DNA adducts in mutagenicity and toxicity of chromium(VI).” *Chem. Res. Toxicol.* **18**:3 –11.